Beam-beam Interaction with a Horizontal Crossing Angle

D.L.Rubin, P.Bagley, M.Billing, J.Byrd, T.Chen, Z.Greenwald, D.Hartill, J.Hylas, J.Kaplan, A.Krasnykh, R.Meller, S.Peck, T.Pelaia, D.Rice, D.Sagan, L.A.Schick, J.Sikora, J.Welch

Abstract

We report measurents of the dependence of luminosity and beam-beam tune shift parameter on horizontal crossing angle at a single interaction point in the Cornell Electron Storage Ring. The report is based on data collected between September 1991 and January 1992 at CESR. For head on collisions (zero crossing angle) the achieved tune shift parameter is $\xi_v = 0.03 \pm 0.002$ at 11ma/bunch. For a crossing half angle of $\theta_c = \pm 2.4mrad$, we achieve $\xi_v = 0.024 \pm 0.002$ at similar bunch currents. Some degradation of performance is observed if the trajectory through the interaction region is distorted magnetically even while head on collisions are preserved. Therefore at least some of the observed dependence of tune shift parameter on crossing angle is due to the associated large displacement of the beam trajectories in the interaction region optics. Furthermore, the algorithm for optimizing luminosity is significantly complicated with the introduction of the crossing angle due to linear optical errors and the solenoid compensation. We have thus demonstrated no fundamental dependence of tune shift parameter on crossing angle but simply identify a lower limit at $\theta_c = 2.4mrad$.

Introduction

In order to store beams with closely spaced bunches and avoid collisions at all but a single interaction point, it is attractive to consider a configuration in which the beams cross at a finite angle. A complication is that a class of synchrobetatron beam-beam resonances can be excited for bunches crossing at an angle that do not appear in the case of head on collisions. The existence of such resonances is confirmed by simulations. We have invented an optical configuration for the CESR storage ring in which a horizontal crossing half angle of $-2.7mrad < \theta_c < 2.7mrad$ is generated by an adjustment of the electrostatic separators, enabling us to explore the effects of the crossing angle on the beam beam interaction and especially the beam-beam tune shift. At the diametrically opposed crossing point the beams are horizontally separated by electrostatic elements independently of the value of the crossing angle and we need consider collisions only at the single interaction point. We can continuously vary the crossing angle over the full range with beams in collision. It is therefore straightforward to interleave measurements of head on conditions throughout the experiment. Note that the crossing angle is so small that the associated geometrical enhancement of the beam size is negligible.

The transverse coupling associated with the experimental solenoid ($B_z = 1.5T$), and its compensation can generate a differential vertical displacement at the interaction point that is proportional to the horizontal displacement of the beams in the interaction region optics. For beams crossing at a horizontal angle there is at CESR no direct measure of the relative displacement at the crossing point. We rely on the beam-beam normal mode tune split to minimize that displacement at finite crossing angle. Indeed such measurements yield information about the errors in the solenoid compensation that are addressed by adjustment of skew quadrupoles located in the vicinity of the interaction point.

Machine Configuration

The quadrupole optics are designed to yield interaction point parameters and betatron and synchrotron tunes similar to those typical of high energy physics operation, since that is where we have the most operating experience. The parameters are summarized in Table I. The "badness" parameter κ is defined as $\kappa = \frac{2\theta_c}{\sigma_x/\sigma_l}$, where θ_c is the crossing half angle, σ_x and σ_l the horizontal and longitudinal beam sizes. κ is a measure of the coupling of synchrotron and betatron motion due to the beams colliding at a finite angle. In the limit of zero bunch length there is no synchrotron motion and therefore no coupling. For a crossing half angle of $\theta_c = 2.5 mrad$ and the machine parameters in the table, $\kappa = 0.184$.

The separation of the beams at the crossing point halfway around the ring from the interaction point is accomplished by suitably arranging the horizontal betatron phase at each of the four electrostatic separators and then powering the separators symmetrically. A similar arrangement of symmetrically powered separators establishes single interaction point conditions for high energy physics luminosity operation. The symmetry axis is the diameter that includes the interaction point. Optimization of the luminosity of head on collisions in the experimental optics proceeds just as for standard machine operation. Also, differences in optical functions and damping partition numbers associated with the horizontal displacement of the beams through the machine arcs, are addressed by the techniques developed for the more traditional CESR lattice. [4] In particular, the vertical separators adjacent to the L3 crossing point can be used to minimize differential vertical displacement and angle of the beams at the crossing point of interest that arise due to lattice errors. The ability to tune the vertical displacement has proven an invaluable tool in the optimization of beam beam performance. Differential horizontal displacement of the two beams in the arcs also provides a means for differential adjustment of the betatron tunes of the two beams via distribution of sextupoles. The optical functions are shown in Figure 1.

The optics are distinguished from standard luminosity optics by the horizontal phase advance from the interaction point to the horizontal separators adjacent to the interaction region. The phase advance in the crossing angle optics is one whole wavelength from the interaction point to the nearest horizontal separator. In standard operating conditions the corresponding phase advance is $\phi_h = \frac{3}{4} \times (2\pi)$. The separators are powered symmetrically to establish the separation at the diametrically opposed crossing point (L3) as shown in Figure 2.

 Table 1. Crossing Angle Lattice Parameters

Q_x	8.57
Q_y	9.63
Q_s°	0.06
eta_x^*	$1.05\mathrm{m}$
eta_u^*	$1.8\mathrm{cm}$
$eta_y^* \ \eta_x^*$	$0.0\mathrm{m}$
σ_l	$1.8\mathrm{cm}$
ϵ_x	$0.24 \times 10^{-6}m - rad$
κ	$0.0735 imes heta_c(mrad)$
Experimental Solenoid	$1.5 \mathrm{Tesla}$
Beam Energy	$5.289 { m GeV}$

Fig. 1. The amplitude and dispersion functions are indicated from the interaction point at the origin to the symmetry point 384.2m away, half way around the ring.

When voltage is superposed asymmetrically on that pair of separators one wavelength from the interaction point, (the pair in the south) a crossing angle is generated. The differential closed orbit through the machine arcs is unaffected by the two wavelength bump with node at the collision point as indicated in Figure 3.

Since the crossing angle appears with the increase of voltage on the east(west) separator and decrease of voltage on the west(east) separator, the maximum angle is attained as the net voltage on the west(east) separator approaches zero. The absolute polarity of the



horizontal separators cannot be changed with stored beam. The technique of superposing the asymmetric voltage necessary to generate the crossing angle on the symmetric value that establishes separation at the parasitic crossing point permits us nevertheless to vary the crossing half angle from nearly -2.7mrad through 0mrad to 2.7mrad with beams in collision. We can therefore explore in a reproducible fashion the horizontal crossing angle dynamics at a single interaction point.

Measured characteristics

Lattice characteristics are verified by measurement. We measure the beta function, local coupling, dispersion, separation at the parasitic crossing point and crossing angle as functions of separator voltage.

1. Measured Optical Functions

The amplitude function β is measured at each of 98 electromagnetic quadrupoles in the CESR lattice. The dependence of betatron tune on magnet current yields the local focusing function. The measurement resolution is such that betatron errors of $\Delta\beta/\beta \geq 0.05$ can be identified. Individual control of all of the machine quadrupoles permits elimination of those errors.

The dependence of orbit displacement on beam energy yields a measure of the dispersion. The horizontal dispersion at the interaction point (nominally zero) is measured to be less than 15cm. The associated energy dependent contribution to the horizontal beam size at the collision point is less than 2%. The vertical dispersion error propagates in the machine arcs with an amplitude of less than 10cm. Extrapolating vertical dispersion measured in the arcs to the interaction point yields $\eta_v^* \leq 2mm$.

We also measure the coupling of horizontal motion into the vertical plane at each of the 98 beam position monitors. The normal mode corresponding most closely to horizontal oscillations is excited externally. The relative phase and amplitude of the resulting vertical component of the motion that is measured can be identified with the dilution of the vertical emittance. In the crossing angle configuration the amplitude of the normalized coupling wave is about 2%, typical of CESR operating conditions.

2. Separation at the Symmetry Point (L3)

In order to determine the relative displacement of the electrons and positrons at the crossing point diametrically opposed from the interaction region we measure an orbit difference. A beam of positrons is stored and we measure the horizontal displacement of the orbit with separators powered symmetrically. We then measure and record the horizontal displacement of the orbit with the separators at zero voltage. The difference of the two horizontal orbits is that part that depends on the separator voltage. The difference is shown in Figure 4. In order to remain in the linear regime of the beam detectors the separators are powered at low voltages so that the displacement is small. Here the voltage

is about 11% of the value used during luminosity measurements. We find the trajectory that best fits the measured difference. The fitted trajectory corresponds to a horizontal displacement $\Delta x = 0.39 \pm 0.02mm$ of the two orbits at the symmetry point. We therefore establish the dependence of the horizontal displacement of the positron beam at the symmetry point on the separator voltage (Δx_{e^+}) . The electrons are displaced in a direction opposite to that of the positrons. $(\Delta x_{e^-} = -\Delta x_{e^+})$ The relative displacement of the beams is $\Delta x_{e^+} + \Delta x_{e^-} = 2\Delta x_{e^+}$. During luminosity measurements the total separation of the beams is $7.02 \pm 0.36mm$.

Fig. 4. Horizontal displacement of the positron beam in each of the 100 beam detectors is measured first with electrostatic separators powered and second with separator voltages at zero. The difference of the two measurements is indicated in the plot. The separator on measurement is with voltages of 11% of the value used during luminosity measurements.

We have assumed that the electron and positron orbits are identical when the separators are at zero voltage, but this is not quite true since the beams travel in opposite directions and therefore there is a beam energy difference that varies with azimuthal coordinate. The energy difference is a consequence of the smooth loss of energy to synchrotron radiation and then the abrupt restoration of that energy in the RF cavities. An orbit difference arises when the energy change occurs in a region of finite dispersion. Because of the symmetry of the guide field and placement of the RF cavities the electron and positron energy difference and the corresponding orbit difference is antisymmetric about the crossing points. The result is a small crossing angle at the symmetry points that is quite independent of the electrostatic separators. There is no contribution to the e^+-e^- displacement at the parasitic crossing point as long as each cavity contributes equally to the energy of each beam. If

there is an error in the relative phase of the RF voltages on the two cavities, then the beams preferentially extract energy from the cavity that attains its peak voltage late. In this case the beams are displaced in opposite directions at the symmetry point. If the phase error is such that all of the energy is extracted from only one of the cavities the separation of the beams at the parasitic crossing point actually increases by about 0.16mm or about 2% of the total.

The measured separation of the beams at the diametrically opposed crossing point corresponds to $N_{\sigma} = \Delta x/\sigma_x = 5.4$. Measurements in standard operating conditions suggest that that separation is adequate to preclude effects on beam lifetime for the regime of beam currents relevant to our experiment. This separation is fixed throughout our luminosity measurements and if the near miss is cause for degradation in beam beam performance it is common to measurements of both finite crossing angle and head on collisions.

Another measure of the effects of the parasitic crossing is in terms of the long range beam beam tune shift. The linear tune shift in the limit of interacting line charges is $\Delta \nu = \frac{r_e N \beta}{2\pi \gamma r^2}$ where r_e is the classical radius of the electron, N the number of particles in the bunch, and r the separation of the centroid of the bunches. For 10ma/bunch and 7.02mm separation, $\Delta \nu_{h/v} = 1 \times 10^{-3}/5.5 \times 10^{-5}$. In so far as the linear tune shift parameter associated with collisions is 0.03-0.035 the effects of the parasitic crossing are negligibly small.

3. Crossing Angle

The optics are designed so that the horizontal separators adjacent to the interaction point will generate a two full wavelength horizontal closed orbit distortion when the separators are powered antisymmetrically. The difference in orbits with separators powered and then at zero voltage is expected to vanish outside of the region of the closed bump. Indeed the residual in the difference is a measure of the phase advance from one separator to the other. The amplitude of the residual is about 1.0mm for a crossing half angle of 2mrad. Therefore, the orbit in the machine arcs shifts by as much as $\pm 1mm$ for electrons and positrons respectively with the introduction of the crossing angle. The observed residual is antisymmetric and does not effect the separation at the parasitic crossing point. The phase error through the interaction region required to generate such a difference in orbits outside of the IR is less than 0.025 betatron wavelengths.

A possible consequence of the error in the horizontal phase between the antisymmetrically powered separators is a relative horizontal displacement of the two beams at the temporal crossing point. If the error in the phase advance is uniformly distributed between the separators the displacement vanishes. If however the error is entirely in the east(west) half of the interaction region a relative displacement of the beams appears at the interaction point of $\Delta_x \leq 0.3 mm\sigma_x/2$. While such a displacement is significant, the phase error can be compensated by the asymmetric adjustment of the individual separator voltages and the beams brought into collision. Luminosity is optimized with respect to that voltage asymmetry and the displacement reduced arbitrarily during the tuning procedure.

We measure a 3mm displacement of the minimum of the beta function from the temporal crossing point. Although this displacement is independent of the crossing angle, we note that it is in general a source of coupling of longitudinal and transverse motion and that the effects of that coupling may depend on the crossing angle.

The crossing angle is determined as was the separation at the parasitic crossing point. The difference in orbits with separators powered symmetrically for separation and antisymmetrically for a crossing angle is recorded. The phase space coordinates of the best fit trajectory are determined. We use only the measurements at the beam detectors within the region of the two full wavelength distortion. We also exclude the four detectors nearest to the interaction point in view of their poorly understood calibration. Ten detectors remain on which to base our determination of the crossing angle.

Alternatively we determine the ratio of horizontal kick to voltage of each of the separators and then compute the crossing angle generated by any given distribution of voltages. The calibration of separator kick is determined by fitting orbit differences based on individually powered separators. In this case we fit a closed orbit with separator kick as parameter. We find that the crossing angles computed in this way are consistent with crossing angles based on the fit to the measured orbits in the interaction region to within a few percent. The determination of the crossing angle is ultimately limited by the detector resolution ^[9] to a level of $\pm 10\%$. For details of the procedure for determining the crossing angle see Chen et. al. ^[10]

The angle measurement based on orbit differences with and without the antisymmetric voltage superimposed on the separators corresponds to that of a single beam and so is correctly identified as the crossing half angle. Differences in the closed orbits of electrons and positrons that arise independently of electrostatic separators must be considered. As noted above such a difference does occur because of the antisymmetric energy difference of the electron and positron beams. The contribution to the crossing half angle for typical CESR parameters (including two RF cavities) is about 0.02mrad, very small compared to the measurement uncertainty. Because the horizontal betatron phase advance from the interaction point to the cavities is very nearly one wavelength, the crossing angle generated by the RF kick is independent of their relative RF phase or voltage.

Luminosity

A significant effort was devoted to tuning the luminosity of head on collisions. Unless our reference is near optimal with respect to a host of effects unrelated to the crossing angle, the dependence on crossing angle is difficult to ascertain. Critical parameters include betatron tunes, differential horizontal and vertical displacement and angle at the interaction point, and transverse coupling. The tune common to both beams and differential tunes are adjusted with quadrupoles and sextupoles in regions of horizontal displacement, respectively. Differential vertical displacement and angle at the interaction point is adjusted with vertical separators located near the parasitic crossing point, and transverse coupling is accessible via some eighteen trim skew quadrupoles. A vertical beam-beam tune shift

parameter of 0.03 ± 0.002 was routinely achieved for head on collisions in the crossing angle optics. (Meanwhile over the stretch of several months during which about 10% of machine time was devoted to crossing angle experiments, continuous tuning of standard luminosity conditions yielded a tune shift parameter of nearly 0.04.)

1. Solenoid Compensation Errors

Three pairs of rotated quadrupoles are used to compensate the transverse coupling introduced by the 1.5 Tesla experimental solenoid. The vertically focusing permament magnet quadrupoles on either side of the interaction point are rotated by about $\pm 5^{\circ}$. The adjacent electromagnetic vertically focusing trim quadrupoles are rotated by $\sim \mp 11^{\circ}$ and the horizontally focusing lenses are rotated by $\pm 2^{\circ}$. The angles are chosen so that there is no coupling of horizontal motion outside of the IR into vertical motion at the interaction point.

The effect of errors in the solenoid compensation is amplified when beams cross at an angle. If compensation is imperfect, the vertical displacement of trajectories at the interaction point is proportional to a linear combination of the horizontal phase space coordinates outside of the interaction region. In the case of head on collisions, the consequence is simply that the vertical beam size at the collision point grows with the horizontal emittance. If in addition there is a finite horizontal angle between the central trajectories of the beams, there will appear a corresponding vertical separation at the interaction point. The determination of the relative displacement of the beams as a function of the crossing angle is a rather precise measure of one component of the coupling matrix.

We measured the ratio of vertical displacement at the interaction point to angle at the horizontal separator as follows. When beams are colliding head on we note luminosity and the normal mode $(\pi - \Sigma)$ splitting of the vertical betatron tune due to the beam beam coupling. The crossing angle is then increased and in general the splitting is reduced as the compensation errors begin to displace the beams vertically. Luminosity and the $\pi - \Sigma$ split is restored by careful adjustment of vertical trim separators and the required vertical separator voltage is noted. We then proceed to larger crossing angles. In order to calibrate the dependence of the vertical displacement on the vertical separator voltage, the horizontal angle is set to zero, and a pair of beam position monitors adjacent to the interaction region are used to measure the relative displacement of the beams as a function of vertical separator voltage. The dependence of vertical displacement on crossing angle measured during the commissioning of the crossing angle optics is shown in Figure 5. The evident linearity is consistent with the hypothesis that the effect is due to compensation errors. The slope is $s \sim 21 \mu m/mrad$ and the $T_{32} = \frac{\partial y}{\partial x'}$ component of the matrix that transports beam from the horizontal separator to the interaction point is given by $T_{32} = s\sqrt{\frac{\beta_{hsep}}{\beta_h^2}} \sim 123.0 \mu m/mrad$. The corresponding beam separation at the interaction point is $5.2\sigma_y$ for a crossing angle $\theta_c = 2mrad$.

It is interesting to consider the consequence of such a coupling error on the vertical beam size. We can estimate the vertical beam size at the interaction point by propagating

Fig. 5. Vertical separation at the crossing point that scales with the horizontal crossing angle is presumed a consequence of solenoid compensation errors before correction.

the horizontal divergence of the beam at the horizontal separator into the vertical. We have that $\sigma_v^* \sim \sqrt{\frac{\epsilon_x}{\beta_{hsep}}} T_{32} = 10.0 \mu m$ which is roughly consistent with the vertical beam size based on the measured luminosity. We conclude that the same compensation error that causes the beams to miss altogether in the event of a horizontal crossing angle has a soft impact on luminosity at beam currents of interest. (Such increases in beam size are presumably observable in a measure of the current dependence of the tune shift parameter even with head on collisions.)

In any event the linear dependence of vertical displacement on crossing angle can be directly related to an element of the coupling matrix. We compute changes to the skew quads in the compensation region consistent with the measured mapping from separator to interaction point but otherwise no change in the coupling outside of the interaction region. Because the quadrupole rotation is somewhat unwieldy, electromagnetic skew quad correction magnets were used to incorporate the changes. The dependence of differential vertical displacement on horizontal crossing angle is reduced by an order of magnitude.

2. Tune shift parameter as a function of crossing angle

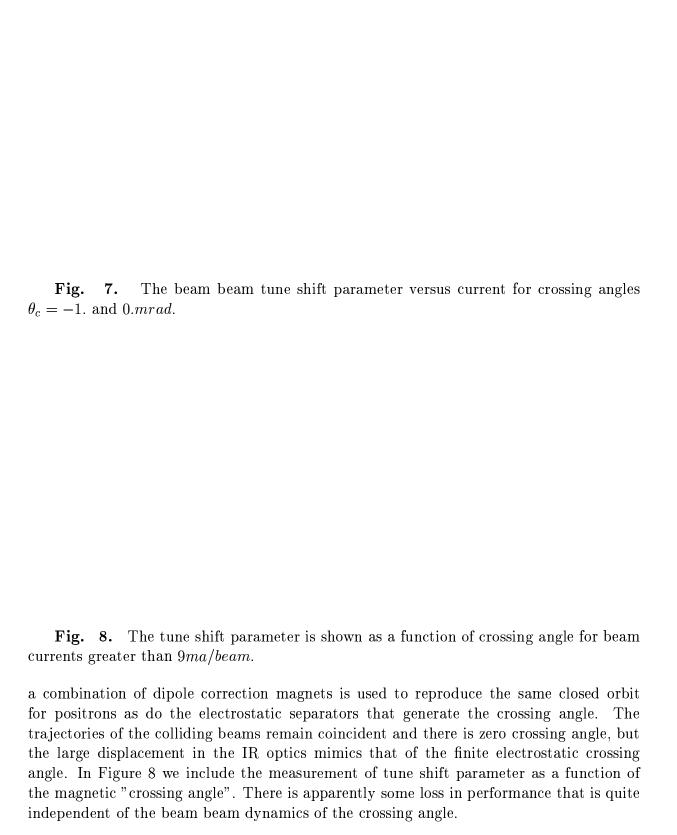
We measure luminosity as a function of the crossing angle over a range of $-2.5 < \theta_c < 2.5 mrad$. θ_c is the crossing half angle. The positive crossing angle corresponds to beams approaching the interaction point from the outside of the ring. Much more time was spent tuning luminosity at negative as opposed to positive crossing angles, so there is probably no significance to the apparent sign dependence. The tune shift parameter is computed from the measured luminosity, beam current and β_v^* . The luminosity is determined from the rate

of Bhabha scattered electrons and positrons into the CLEO detector end cap calorimeter. The variation among points at any given crossing angle reflects counting statistics, ($\pm 5 - 10\%$), and the inevitable tuning. The luminosity monitor is periodically cross calibrated with wide angle data. Corrections at the few percent level are typical. There was no such cross calibration specifically with crossing angle data. But the acceptance of the detector is such that the effect of the crossing angle is expected to have negligible impact on luminosity monitor performance. All luminosity data are collected when beam lifetime is in excess of 30 minutes. The current dependence of the tune shift parameter is indicated in Figure 6 for crossing half angles $\theta_c = -2.5, 0.$, and 2.5mrad. Uncertainty in the angle is $\pm 5 - 10\%$. Data for $\theta_c = -1, 0$, and 1mrad are shown in Figure 7.

Fig. 6. The beam beam tune shift parameter is plotted as a function of beam current for collisions at three different crossing angles. ($\theta_c = -2.5, 0.$, and +2.5mrad) The tune shift parameter is based on the measured luminosity and beam current. The statistical uncertainty in the measured luminosity is small compared to fluctuations from point to point associated with tuning.

The dependence of tune shift parameter on crossing angle is shown in Figure 8. We include only measurements at currents greater than 9ma/beam. Figures 6 and 7 suggest that the tune shift parameter saturates near 9ma per bunch and that beyond 9ma the tune shift parameter is roughly independent of current. We believe that the effects of the residual solenoid compensation errors are small. At each crossing angle luminosity is optimized with respect to vertical and horizontal displacements at the interaction point by adjustment of vertical trim separators, as well as the horizontal separators. The tuning procedure is nevertheless complicated by the existence of the crossing angle. For example, skew quad adjustements tend to change the closed orbit as well as the beam size.

We anticipate the possibility that the large displacement of the beams in the interaction region optics may effect the beam beam performance. In order to quantify the effect,



3. Dynamics of Particles at large Amplitudes

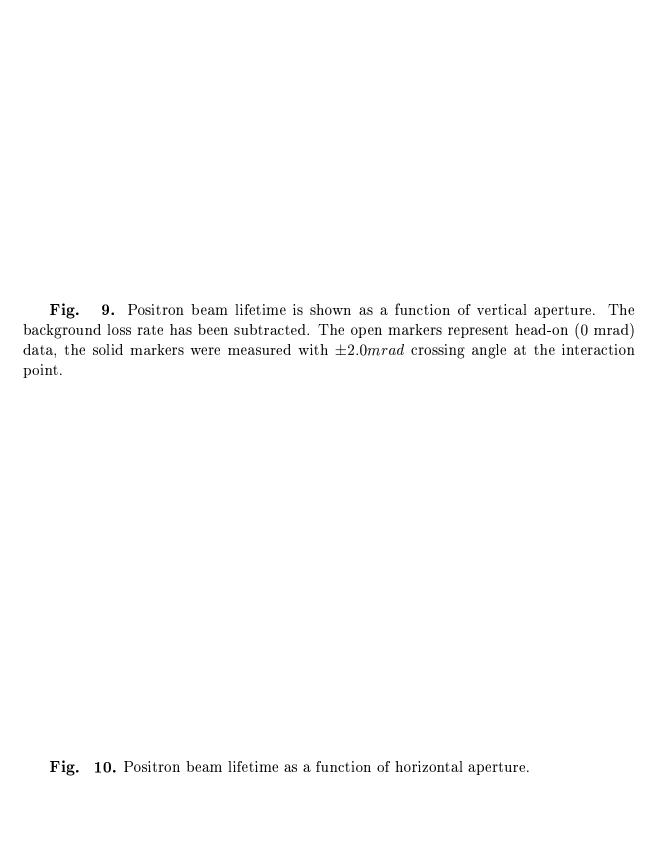
The beam beam tune shift parameter ξ_v characterizes the effects of the beam beam interaction on the bunch core and so reflects small amplitude behavior. The distribution of particles at larger amplitudes determines the beam lifetime and detector background. In an effort to identify the effect of crossing angle on the particles far from the core of the beam we measure the large amplitude particle density for both head on collisions ($\theta_c = 0mrad$) and finite crossing angle ($\theta_c = \pm 2mr$). The experimental technique used to determine the particle distribution at large amplitudes is to monitor beam lifetime while varying a local transverse aperture. The initial particle loss rate is subtracted from each measurement to determine the loss from the local aperture. Since synchrotron radiation determines the rate of change of a particle's amplitude and a state of equilibrium between the radiation damping and excitation exists, the transverse distribution is gaussian and the lifetime is given by:

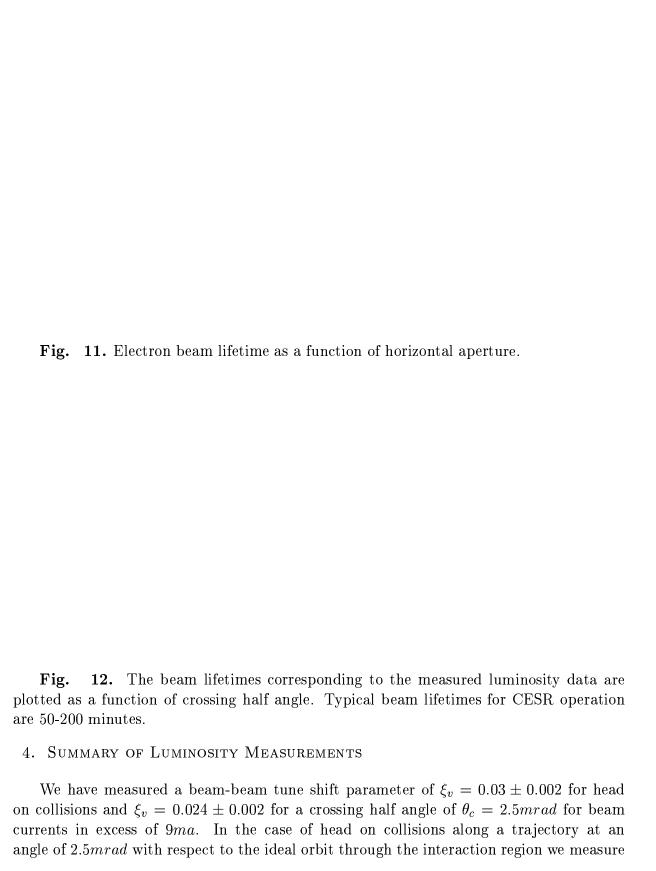
$$\tau = \frac{\tau_q}{2} \frac{2\sigma_x^2}{X_{ap}^2} \exp\left(\frac{X_{ap}^2}{2\sigma_x^2}\right)$$

where τ_q is the transverse damping time, X_{ap} the distance of the aperture from the beam centerline, and σ_x is the rms beam size. X_{ap} and σ_x refer to horizontal aperture and beam size or vertical aperture and beam size. Measurements of large amplitude particle distribution were made during crossing angle machine studies. We compare the results taken with a $\pm 2.0mr$ crossing angle with head on collisions in otherwise similar machine conditions. If the particle distribution is gaussian than we expect that a plot of the log of the lifetime as a function of of the distance of a movable aperture ("scraper") from the beam centerline will produce an approximately straight line. The vertical scraper measurement results are shown in Figure 9. Data from head-on conditions are shown with open points, and crossing angle data are shown in solid points. While significant non-gaussian growth of the beam "tails" is evident in both 0.0 and 2.0 mrad data, no additional amplitude increase can be attributed to the horizontal crossing angle.

The horizontal scraper data for positrons are shown in Figure 10. In this case, a clear increase in beam size is apparent in the 9 mA data. The 11 mA data, however, taken with a slightly different betatron tune, show a clear decrease in large amplitude particle distribution when the crossing angle is turned on. Similar measurements for electrons, shown in Figure 11, show a smaller increase in beam size with crossing angle for both 9 amd 11 mA data sets. A sensitivity to tune of beam tails in crossing angle conditions is expected. At the two tunes chosen for these measurements, the tune dependence is much more obvious in the positron data than the electron data. In any case, the increase in the apparent beam size at large amplitudes for collisions with the crossing angle as compared to head on collisions is no more than approximately 10%.

Finally, the beam lifetimes recorded simultaneously with each measurement of the tune shift parameter (Figures 6 and 7) are summarized in Figure 12. There is no significant dependence of beam lifetime on crossing angle.





 $\xi_v = 0.027 \pm 0.002$. We conclude that large orbit distortions in the interaction region quadrupoles are not readily compensated. (Displacement in the final horizontally focusing quadrupole is $\pm 2.2cm$ for a crossing angle $\theta_c = 2.5mrad$.). At each point the luminosity is optimized with respect to betatron tune, differential tune and differential closed orbits. The deterioration of performance with crossing angle is clear, while the cause of that deterioration is not. There are several effects peculiar to beams crossing at an angle that are not fundamental to the beam beam interaction, including an enhanced sensitivity to solenoid compensation errors, large displacements in the interaction region optics, and a more complicated tuning optimization. Skew quad adjustments tend to shift electron and positron closed orbits in opposite directions. Also, as previously noted there is a small shift in the closed orbits of the electrons and positrons in the machine arcs with the introduction of the crossing angle due to optical errors. Because of the sextupole nonlinearities the shifting orbit may have some effect on the beam beam dynamics. Again the tuning algorithm for the optimization of luminosity is complicated. The optical errors may likewise lead to a differential displacement of the beams at the interaction point and while the individual control of the separator voltages can in principle eliminate the difference, convergence via tuning to optimal performance is practically reduced. The differences in performance are small enough to suggest that with sufficient attention to optical errors etc., good luminosity can be achieved with beams crossing at an angle $\theta_c \leq$ 2.5mrad.

Acknowledgement

We would like to acknowledge the extraordinary efforts of the CESR operators and to the CESR operations group in helping to make this study successful.

REFERENCES

- D. Sagan, R. Siemann, and S. Krishnagopal, 2nd Europ. Part. Acc. Conf., p. 1649 (1990).
 A. Piwinski, IEEE Trans. Nuc. Sci., NS-24, No. 3 p. 1408 (1981).
 A. Piwinski, IEEE Trans. Nuc. Sci., NS-32, No. 5, p. 2240 (1985).
 A. Piwinski, SSC-57 (1986).
- 2. L.A.Schick, Horizontal Crossing Angle Machine Studies, CON 91-2.
- 3. David Sagan, Cornell CBN 91-01 (1991).
- D.L.Rubin and L.A.Schick, Single Interaction Point Operation of CESR, Proceedings of the 1991 Particle Accelerator Conference, San Francisco, California, May 1991, pp. 144-146
- 5. J.Sikora and R.Littauer, Monitoring System to Permit Accurate Alignment of Beams at the Collision Point in CESR, Proceedings of the 1991 Particle Accelerator Conference, San Francisco, California, May, 1991
- 6. P.Bagley and D.Rubin, Correction of Transverse Coupling in CESR, Proceedings the 1989 Particle Accelerator Conference, Chicago, Illinois, p.

- 7. R.Littauer, Orbit and Tune Effects of RF Conditions, CBN 884, August 1989.
- 8. D.Rice, Multibunch Pretzel Separation Measurements in CESR, 1/13/92
- 9. P.Bagley and G.Rouse, "Calibration of a Beam Position Detector By Moving the Beam Pipe", CBN 91-17, December, 1991
- T.Chen, T.Pelaia, and D.Rubin, Calibration of Crossing Angle, internal memo, May, 1992
- 11. A. Piwinski, IEEE Trans. Nuc. Sci., **NS-24**, No. 3 p. 1408 (1981). A. Piwinski, IEEE Trans. Nuc. Sci., **NS-32**, No. 5, p. 2240 (1985). A. Piwinski, SSC-57 (1986).
- 12. T.Chen, PhD Thesis

FIGURE CAPTIONS

- 1. The amplitude and dispersion functions are indicated from the interaction point at the origin to the symmetry point half way around the ring
- 2. The symmetric closed orbit distortion through the entire ring yields head on collisions at the interaction point at left and right boundaries of the plot. The beams are separated at the parasitic crossing point half way around the arcs which appears at the midpoint of the figure.
- 3. The asymmetric superposition of voltage on the separators that straddle the interaction region generates a horizontal crossing angle at the interaction point while preserving the symmetric separation throughout the arcs.
- 4. Horizontal displacement of the positron beam in each of the 100 beam detectors is measured first with electrostatic separators powered and second with separator voltages at zero. The difference of the two measurements is indicated in the plot.
- 5. Vertical separation at the crossing point that scales with the horizontal crossing angle is presumed a consequence of solenoid compensation errors.
- 6. The beam beam tune shift parameter is plotted as a function of beam current for collisions at three different crossing angles. ($\theta_c = -2.5, 0.$, and +2.5mrad) The tune shift parameter is based on the measured luminosity and beam current. The statistical uncertainty in the measured luminosity is indicated for a single point.
- 7. The beam beam tune shift parameter versus current for crossing angles $\theta_c = -1$. and 0.mrad.
- 8. The tune shift parameter is shown as a function of crossing angle for beam currents greater than 9ma/beam.
- 9. Positron beam lifetime is plotted as a function of vertical aperture. The background loss rate is subtracted. The open markers represent head-on (0 mrad) data, the solid markers were measured with $\pm 2.0 mrad$ crossing angle at the interaction point.
- 10. Positron beam lifetime is indicated as a function of horizontal aperture.
- 11. Electron beam lifetime as a function of horizontal aperture.

10	The beam	lifatimes correspond	ing to the	mangurad l	uminosity dat	e ere plotted as
12.		lifetimes correspond of crossing half ang tutes.	~		=	-